

8. Supplementary Materials

8.1. Additional Tables and Figures for the Analysis

856 (6.9)	867 (8.4)	846 (7.9)	834 (10.6)	953 (21.5)
937 (19.7)	945 (16.9)	929 (16.1)	920 (15.0)	960 (15.5)
750 (6.3)	765 (6.6)	738 (4.7)	724 (5.2)	699 (4.1)
803 (7.5)	815 (7.5)	790 (9.4)	777 (6.8)	684 (4.4)
897 (13.2)	907 (13.3)	887 (13.0)	876 (12.0)	678 (3.1)

Table 3: Hyperspectral pixel, represented as physical 2D-grid of peak bands in nm and width half-peak-full-width specified between brackets in nm of the near-infrared sensor (H1).

538 (12.9)	552 (13.0)	524 (9.2)	512 (6.5)
620 (5.1)	480 (6.6)	611 (12.2)	602 (12.1)
580 (10.7)	591 (11.4)	567 (11.0)	554 (11.7)
489 (10.6)	500 (8.2)	477 (7.9)	470 (2.9)

Table 4: Hyperspectral pixel, represented as physical 2D-grid of peak bands in nm and width half-peak-full-width specified between brackets in nm of the visual sensor (H2).

For reference, tables are included that depict exact numbers instead of bar charts. Table 5 corresponds to fig. 6, while table 6 matches fig. 9

8.2. Shutter time and Gain Compensation Details

The shutter time and gain values are automatically determined by the camera to achieve higher dynamic range, especially in low-light conditions. Consequently, the resulting image data have to be rescaled to the same scale. This is done using the following transformation:

$$q = \frac{p}{r_c(s - x_0) + y_0} \quad (4)$$

Where q is the transformed version of pixel value p , with shutter time s . The other values depend upon the camera used and gain setting. The values are listed in table 7. These were obtained by maintaining the same light intensity, while varying and camera configuration. Transforming these using eq. (4), results in a constant value.

Table 5: Performance of the linear model for different eco-physiological and environmental parameters. The lower the NMSE, the better. \times means that the model was trained without the vegetation indices (VI), while VI indicates that they were included. This table provides the same information as fig. 6 but in a different form.

task	plant1		plant2		wood		PVC		Ytong		cotton	
	\times	VI	\times	VI	\times	VI	\times	VI	\times	VI	\times	VI
P_n	0.301	0.206	0.556	0.56	0.523	0.34	0.395	0.34	0.585	0.625	0.589	0.587
g_s	0.676	0.653	0.958	0.957	0.913	0.634	0.693	0.649	0.977	1.006	0.99	1.002
Tr	0.426	0.408	0.597	0.602	0.5	0.309	0.4	0.353	0.647	0.656	0.656	0.646
VPD_{leaf}	0.18	0.107	0.277	0.233	0.214	0.135	0.201	0.156	0.285	0.252	0.31	0.277
T_{leaf}	0.052	0.027	0.07	0.035	0.052	0.034	0.064	0.031	0.092	0.048	0.088	0.041
T_{air}	0.081	0.02	0.068	0.044	0.134	0.124	0.164	0.1	0.121	0.075	0.109	0.062
RH	0.432	0.297	0.382	0.439	0.478	0.371	0.466	0.436	0.631	1.132	0.356	0.325
PAR	0.025	0.018	0.03	0.039	0.024	0.016	0.021	0.015	0.029	0.03	0.028	0.027

Table 6: Overview of performance for all variables for a subsample size of 77 (30+47), resulting in 1502 input features for the model. Mean (\bar{y}) and standard deviation (σ) columns provide the same information as fig. 9 in table form.

task	plant1		plant2		wood		PVC		Ytong		cotton	
	\bar{y}	σ	\bar{y}	σ	\bar{y}	σ	\bar{y}	σ	\bar{y}	σ	\bar{y}	σ
P_n	0.262	0.039	0.574	0.039	0.271	0.032	0.282	0.029	0.55	0.011	0.544	0.014
g_s	0.613	0.046	0.854	0.046	0.668	0.023	0.701	0.022	0.923	0.008	0.914	0.015
Tr	0.451	0.04	0.51	0.032	0.411	0.008	0.419	0.014	0.637	0.01	0.671	0.011
VPD_{leaf}	0.217	0.035	0.352	0.019	0.222	0.009	0.217	0.012	0.349	0.006	0.402	0.024
T_{leaf}	0.057	0.01	0.138	0.041	0.052	0.003	0.066	0.001	0.115	0.019	0.109	0.004
T_{air}	0.11	0.028	0.151	0.048	0.103	0.015	0.101	0.007	0.159	0.03	0.142	0.005
RH	0.432	0.066	0.684	0.125	0.421	0.038	0.32	0.023	0.616	0.04	0.574	0.022
PAR	0.026	0.001	0.028	0.001	0.02	0	0.022	0	0.026	0	0.027	0

camera	gain	r_c	x_0	y_0
NIR	0	0.1216	7,200	1,454
NIR	12	0.1216	7,200	3,478
VIS	0	0.1301	7,200	2,213
VIS	12	0.1301	7,200	4,004

Table 7: Correction values for shutter time and gain compensation.

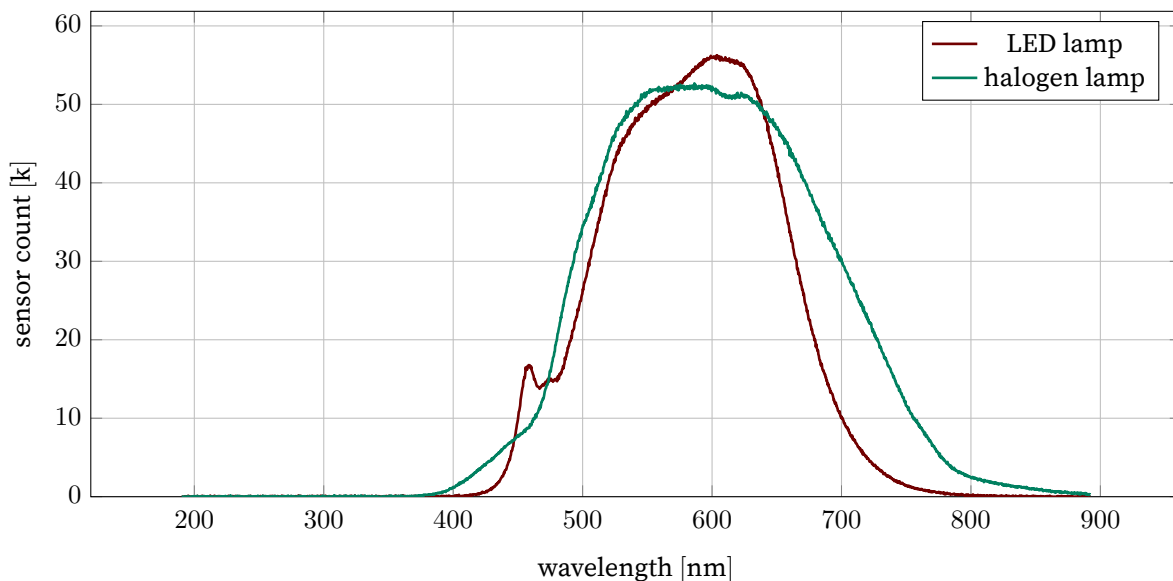


Figure 11: Spectrum of the halogen lights and LED lights used in the experiments. The spectral were measured using Jaz Spectrometer (Ocean Optics, Dunedin, FL, USA) from a distance of 20 cm directly below the light source.

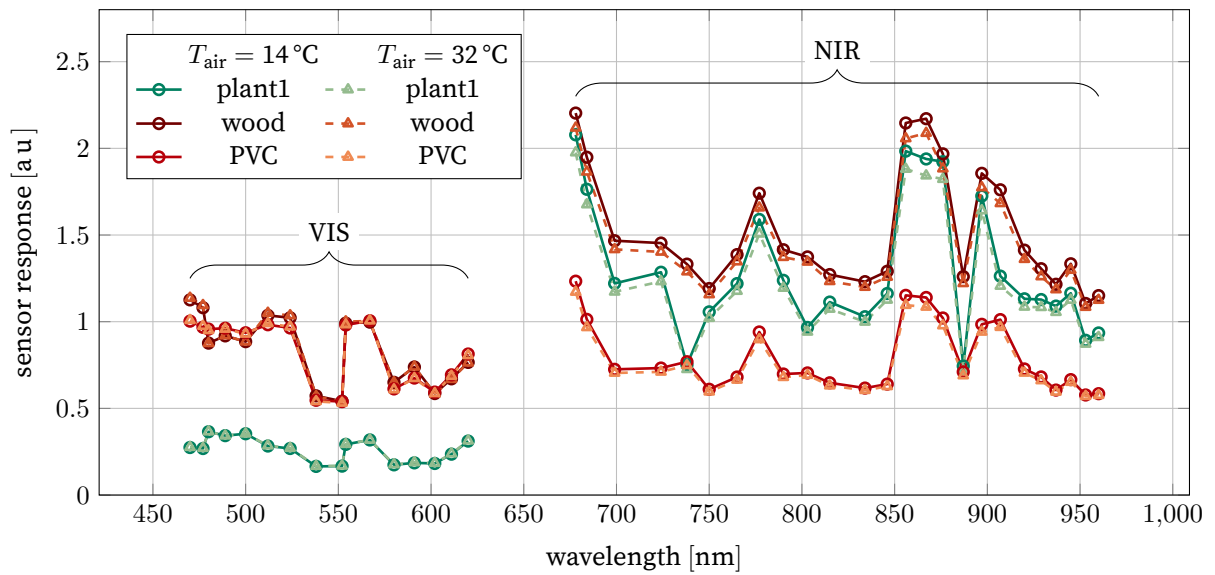


Figure 12: Reflection spectra of the three materials in the first experiments at similar PAR conditions ($200 \mu\text{mol m}^{-2} \text{s}^{-1}$) at two different temperatures, $T_{\text{air}} = 14^\circ\text{C}$ and $T_{\text{air}} = 32^\circ\text{C}$, illustrating the variable spectral response. The peaking of some peaks is the result of strong secondary peaks of the sensor's response and the emission spectra of the lights, depicted in fig. [11](#)